Electronic Supplementary Material (ESI) for Journal of Materials Chemistry C.

Enhanced Energy Migration Strategy in Upconverting Nanocrystals:

Color-Tuning with High Quantum Yield.

Damien Hudry,[1] Dmitry Busko,[1] Radian Popescu,[2] Dagmar Gerthsen,[2] Ian Howard,[1,3] Bryce Richards[1,3]

1 Institute of Microstructure Technology, Karlsruhe Institute of Technology, Hermann-von-Helmholtz-Platz 1, D-76344 Eggenstein-Leopoldshafen, Germany.

2 Laboratory of Electron Microscopy, Karlsruhe Institute of Technology, Engesserstrasse 7, D-76131 Karlsruhe, Germany.

3 Université Grenoble Alpes, CNRS, Institut Néel, 38000 Grenoble, France.

3 Light Technology Institute, Karlsruhe Institute of Technology, Engesserstrasse 13, D-76131 Karlsruhe, Germany.

Supporting Information

Content

1. Chemicals.

Oleic acid (OA, technical grade, 90%), octadecene (ODE, technical 90%), sodium hydroxide (NaOH, anhydrous, 98%), ammonium fluoride (NH_4F, 99.99%), sodium trifluoroacetate (98%) anhydrous methanol (MeOH), absolute ethanol (EtOH), and toluene ($C_6H_5CH_3$) were purchased from Sigma Aldrich and were used without further purification. Note that sodium hydroxide, ammonium fluoride, anhydrous methanol, OA, and ODE are stored under inert conditions in a glovebox under dry nitrogen (O_2 < 1 ppm, H_2O < 1 ppm). Note that all given quantities for rare earth acetate precursors were corrected based on their corresponding thermogravimetric analyses.

2. Synthesis of rare earth acetates.

Synthesis of Gd(OOCCH$_3$)$_3$. $Gd(OOCCH_3)_3$ was prepared by adding 10 mmol of gadolinium oxide (Gd_2O_3) to 6.2 mL of glacial acetic acid and 12.4 mL of deionized water in a 50 mL round bottom flask equipped with a reflux condenser. The stirred suspension was heated up to 90°C under air until the solid oxide was completely dissolved and a clear colorless solution was obtained (14 hours, 90°C). After cooling, the solution was filtered and the solvent evaporated with a rotary evaporator at 60°C for 90 min. The obtained wet powder was dried under vacuum at 60°C for 6 hours. The dry powder was stored under inert conditions in a glovebox under dry nitrogen (O_2 < 1 ppm, H_2O < 1 ppm). Note that the compound obtained was slightly hydrated as shown with its corresponding thermogravimetric analysis.

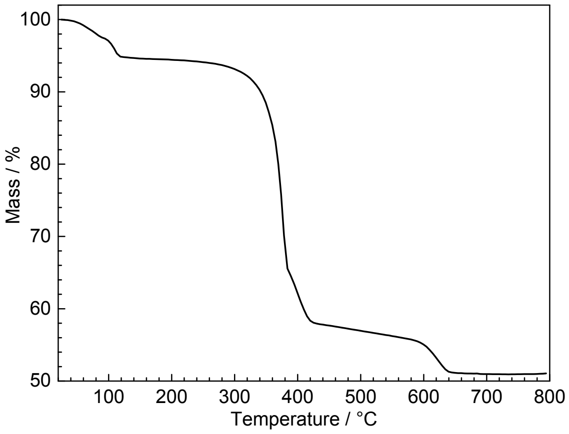

Thermogravimetric analysis of the as-prepared gadolinium acetate performed under argon with a heating rate of 10°C.min^{-1}.

Synthesis of Er(OOCCH$_3$)$_3$. Er(OOCCH$_3$)$_3$ was prepared by adding 10 mmol of erbium oxide (Er$_2$O$_3$) to 6.2 mL of glacial acetic acid and 12.4 mL of deionized water in a 50 mL round bottom flask equipped with a reflux condenser. The stirred suspension was heated up to 90°C under air until the solid oxide was completely dissolved and a clear pinkish solution was obtained (14 hours, 90°C). After cooling, the solution was filtered and the solvent evaporated with a rotary evaporator at 60°C for 90 min. The obtained wet powder was dried under vacuum at 60°C for 6 hours. The dry powder was stored under inert conditions in a glovebox under dry nitrogen (O_2 < 1 ppm, H_2O < 1 ppm). Note that the compound obtained was anhydrous as shown with its corresponding thermogravimetric analysis.

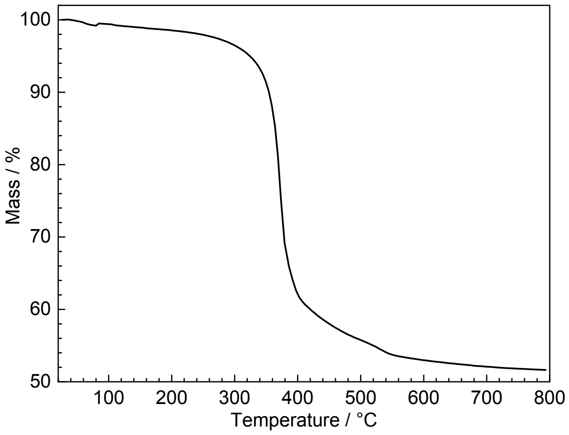

Thermogravimetric analysis of the as-prepared erbium acetate performed under argon with a heating rate of 10°C.min^{-1}.

3. Synthesis of rare earth trifluoroacetates.

Synthesis of Y(OOCCF$_3$)$_3$. Y(OOCCF$_3$)$_3$ was prepared by adding 10 mmol of yttrium oxide (Y$_2$O$_3$) to 6.2 mL of trifluoroacetic acid and 12.4 mL of deionized water in a 50 mL round bottom flask equipped with a reflux condenser. The stirred suspension was heated up to 90°C under air until the solid oxide was completely dissolved and a clear colorless solution was obtained (14 hours, 90°C). After cooling, the solution was filtered and the solvent evaporated with a rotary evaporator at 60°C for 90 min. The obtained wet powder was dried under vacuum at 60°C for 6 hours. The dry powder was stored under inert conditions in a glovebox under dry nitrogen (O_2 < 1 ppm, H_2O < 1 ppm). Note that the compound obtained was slightly hydrated as shown with its corresponding thermogravimetric analysis.

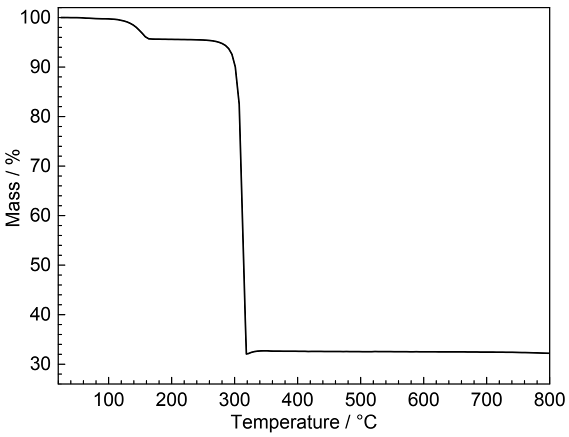

Thermogravimetric analysis of the as-prepared yttrium trifluoroacetate performed under argon with a heating rate of 10°C.min^{-1}.

Synthesis of $Gd(OOCCF_3)_3$. $Gd(OOCCF_3)_3$ was prepared by adding 10 mmol of gadolinium oxide (Gd_2O_3) to 6.2 mL of trifluoroacetic acid and 12.4 mL of deionized water in a 50 mL round bottom flask equipped with a reflux condenser. The stirred suspension was heated up to 90°C under air until the solid oxide was completely dissolved and a clear colorless solution was obtained (60 min, 90°C). After cooling, the solvent was evaporated with a rotary evaporator at 60°C for 60 min. The obtained wet powder was dried under vacuum at 60°C for 17 hours. The dry powder was stored under inert conditions in a glovebox under dry nitrogen (O_2 < 1 ppm, H_2O < 1 ppm). Note that the compound obtained was hydrated as shown with its corresponding thermogravimetric analysis.

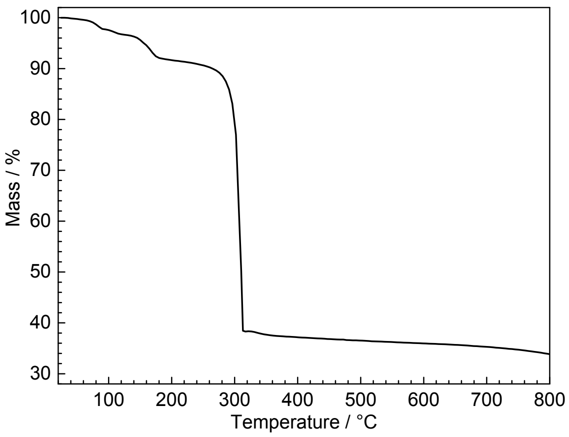

Thermogravimetric analysis of the as-prepared gadolinium trifluoroacetate performed under argon with a heating rate of 10°C.min^{-1}.

Synthesis of $Tm(OOCCF_3)_3$. $Tm(OOCCF_3)_3$ was prepared by adding 10 mmol of thulium oxide (Tm_2O_3) to 6.2 mL of trifluoroacetic acid and 12.4 mL of deionized water in a 50 mL round bottom flask equipped with a reflux condenser. The stirred suspension was heated up to 90°C under air until the solid oxide was completely dissolved and a clear colorless solution was obtained (24h, 90°C). After cooling, the solvent was evaporated with a rotary evaporator at 60°C for 60 min. The obtained wet powder was dried under vacuum at 60°C for 6 hours. The dry powder was stored under inert conditions in a glovebox under dry nitrogen (O_2 < 1 ppm, H_2O < 1 ppm). Note that the compound obtained was slightly hydrated as shown with its corresponding thermogravimetric analysis.

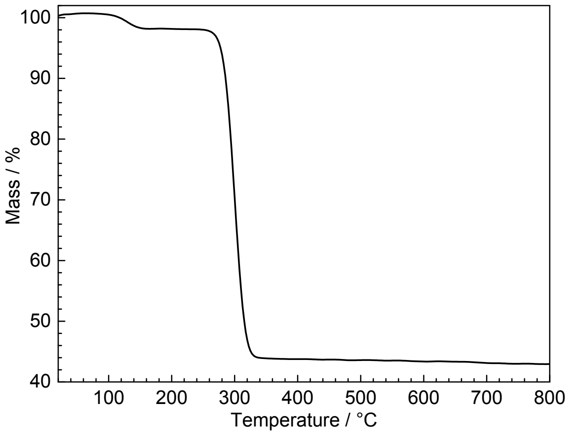

Thermogravimetric analysis of the as-prepared thulium trifluoroacetate performed under argon with a heating rate of 10°C.min^{-1}.

Synthesis of $Yb(OOCCF_3)_3$. $Yb(OOCCF_3)_3$ was prepared by adding 10 mmol of ytterbium oxide (Yb_2O_3) to 6.2 mL of trifluoroacetic acid and 12.4 mL of deionized water in a 50 mL round bottom flask equipped with a reflux condenser. The stirred suspension was heated up to 90°C under air until the solid oxide was completely dissolved and a clear colorless solution was obtained (18h, 90°C). After cooling, the solvent was evaporated with a rotary evaporator at 60°C for 60 min. The obtained wet powder was dried under vacuum at 60°C for 15 hours. The dry powder was stored under inert conditions in a glovebox under dry nitrogen (O_2 < 1 ppm, H_2O < 1 ppm). Note that the compound obtained was slightly hydrated as shown with its corresponding thermogravimetric analysis.

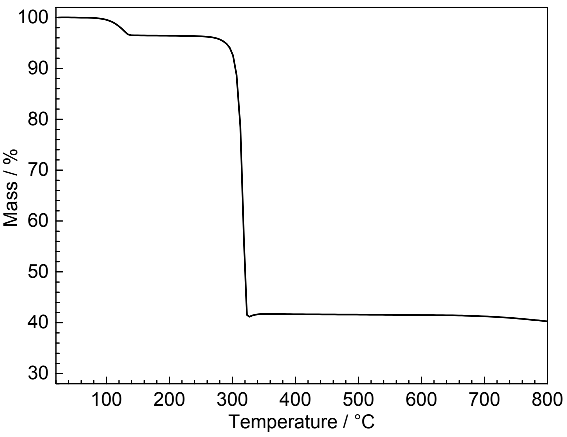

Thermogravimetric analysis of the as-prepared ytterbium trifluoroacetate performed under argon with a heating rate of 10°C.min^{-1}.

4. Synthesis of core upconverting nanocrystals.

Synthesis of β-NaEr$_{0.8}$Yb$_{0.2}$F$_4$ core nanocrystals (NCs). β-NaGd$_{0.98}$Er$_{0.02}$F$_4$ was synthesized by the method that was first reported by Li and Zhang.[1] The synthesis has been slightly modified compared to the experimental procedure published by Wang and co-workers.[2] The synthesis was performed using air-free techniques (Schlenk line and glovebox) under purified nitrogen (glovebox) or argon (Schlenk line).

Note that all β-NaGd$_{0.98}$Er$_{0.02}$F$_4$ core NCs obtained from one single batch synthesis will be used as the starting seeds for the subsequent growth of triple-shell (CS3$_x$ with x = I, II, or III) upconverting NCs (see section 6).

Preparation of solution A. Gd(OOCCH$_3$)$_3$ (4.0 mmol) and Er(OOCCH$_3$)$_3$ (0.1 mmol) are introduced in a 250 mL round bottom flask together with OA (40 mL) and ODE (60 mL). The resulting mixture is heated up to 140°C (under Ar) to dissolve lanthanide acetates. The white turbid solution turns to an optically clear slightly yellowish solution within twenty minutes at 140°C. Then, the temperature is decreased to 100°C, and the optically clear solution is purified under vacuum. The vacuum purification consists in ten Ar ↔ vacuum (2.0.10^{-1} to 4.0.10^{-2} mbar) cycles followed by a dynamic vacuum step (1.0.10^{-3} mbar) for 10 minutes. The resulting solution (solution A) is kept under static Ar and cooled down to room temperature (25°C).

Preparation of solution B. In a dry glovebox under N_2, two methanol solutions are prepared in two 50 mL centrifuge tubes. First, 10.3 mmol of NaOH are introduced in the first 50 mL centrifuge tube with 15 mL of anhydrous MeOH. Second, 16.4 mmol of NH_4F are introduced in the second 50 mL centrifuge tube with 30 mL of anhydrous MeOH. After complete dissolution (≈ 15 min), both centrifuge tubes are removed from the glovebox. Solution B is obtained by injecting the methanol solution of NaOH into the methanol solution of NH_4F. Note that solution B is prepared just before its injection into solution A.

Synthesis of β-$NaGd_{0.98}Er_{0.02}F_4$ core NCs. Solution B is immediately injected into solution A under Ar. The resulting solution is heated up to 50°C under Ar. The temperature is maintained for 30 minutes and then MeOH is evaporated under reduced pressure - 5.10^{-3} mbar for 30 minutes. Once MeOH is completely evaporated, the resulting solution is heated up under Ar to 280°C for 90 min. Then, the heating mantle is removed, and the flask is left to cool naturally to room temperature.

Extraction and purification of β-$NaGd_{0.98}Er_{0.02}F_4$ core NCs. The raw solution (100 mL) is split into five (5x50 mL) centrifuge tubes (≈ 20 mL of raw solution per tube). After centrifuging (3000xg, 5 min) a clear slightly yellowish supernatant and white precipitate are obtained in each centrifuge tubes. For each centrifuge tube, the supernatant is discarded and the resulting white precipitate is dispersed in toluene (2 mL) to give a clear colorless solution. Solutions obtained from the five centrifuge tubes are combined into a single unique centrifuge tube. Nanocrystals are purified by adding 30 mL of acetone. The solution immediately turns white turbid. After centrifuging (3000xg, 3 min) a clear colorless supernatant and white precipitate are obtained. The supernatant is discarded and the resulting white precipitate is dispersed in toluene (10 mL) to give a clear colorless solution. The purification procedure (precipitation with acetone, centrifuging, and toluene dispersion) is repeated three times. After the final dispersion step in toluene, the solution is centrifuge at 3000xg for 3 minutes to remove all residual insoluble.

Purified β-$NaGd_{0.98}Er_{0.02}F_4$ core NCs dispersed in 10 mL toluene are stored in a tightly closed glass vial. This constitutes the unique stock solution of optically active seeds for the subsequent synthesis of $CS3_x$ upconverting NCs.

5. Synthesis of shell precursor solutions.

Sodium shell precursor solution (NaTFA). The shell precursor solution NaTFA is prepared by introducing $NaOOCCF_3$ (3 mmol) into a 50 mL round bottom flask together with OA (15 mL) and ODE (15 mL). The resulting mixture is heated up to 120°C (under Ar) to dissolve the trifluoroacetate. The white turbid solution turns to an optically clear slightly yellowish solution within few minutes at 120°C. After 15 minutes, the temperature is decreased to 100°C, and the optically clear solution is purified under vacuum (five argon / vacuum dynamic steps at $5.0.10^{-2}$ mbar and 10 minutes under static vacuum at 10^{-3} mbar). The resulting solution is transferred into a dry glovebox under N_2 where it can be safely stored. **The final Na concentration is 0.1 mmol/mL.**

Ytterbium shell precursor solution (YbTFA). The shell precursor solution YbTFA is prepared by introducing $Yb(OOCCF_3)_3$ (1.5 mmol) into a 50 mL round bottom flask together with OA (7.5 mL) and ODE (7.5 mL). The resulting mixture is heated up to 120°C (under Ar) to dissolve the trifluoroacetate. The white turbid solution turns to an optically clear slightly yellowish solution within few minutes at 120°C. After 15 minutes, the temperature is decreased to 100°C, and the optically clear slightly yellowish solution is purified under vacuum (same purification procedure as for NaTFA shell precursor solution). The resulting solution is transferred into a dry glovebox under N_2 where it can be safely stored. **The final Yb concentration is 0.1 mmol/mL.**

Gadolinium/thulium shell precursor solution (GdTmTFA). The shell precursor solution GdTmTFA is prepared by introducing $Gd(OOCCF_3)_3$ (1.485 mmol) and $Tm(OOCCF_3)_3$ (0.015 mmol) into a 50 mL round bottom flask together with OA (7.5 mL) and ODE (7.5 mL). The resulting mixture is heated up to 120°C (under Ar) to dissolve the trifluoroacetates. The white turbid solution turns to an optically clear slightly yellowish solution within few minutes at 120°C. After 15 minutes, the temperature is decreased to 100°C, and the optically clear slightly yellowish solution is purified under vacuum (same purification procedure as for NaTFA shell precursor solution). The resulting solution is transferred into a dry glovebox under N_2 where it can be safely stored. **The final lanthanide (ΣGd, Tm) concentration is 0.1 mmol/mL.**

Yttrium shell precursor solution (YTFA). The shell precursor solution YTFA is prepared by introducing $Y(OOCCF_3)_3$ (1.5 mmol) into a 50 mL round bottom flask together with OA (7.5 mL) and ODE (7.5 mL). The resulting mixture is heated up to 120°C (under Ar) to dissolve the trifluoroacetate. The white turbid solution turns to an optically clear slightly yellowish solution within few minutes at 120°C. After 15 minutes, the temperature is decreased to 100°C, and the optically clear slightly yellowish solution is purified under vacuum (same purification procedure as for NaTFA shell precursor solution). The resulting solution is transferred into a dry glovebox under N_2 where it can be safely stored. **The final Y concentration is 0.1 mmol/mL.**

6. Synthesis of triple-shell upconverting nanocrystals.

Synthesis of β-$NaGd_{0.98}Er_{0.02}F_4$/$NaYbF_4$ single-shell NCs (CS_x). β-$NaEr_{0.8}Yb_{0.2}F_4$/$NaYbF_4$ NCs were synthesized by the controlled hot injection method.

Seeds solution. The seeds solution is prepared by introducing β-$NaEr_{0.8}Yb_{0.2}F_4$ stock solution (Table 1) into a 50 mL round bottom flask together with OA (4 mL) and ODE (4 mL). The resulting mixture is heated up to 100°C (under Ar) and purified under vacuum. The vacuum purification consists in fifteen Ar ↔ vacuum ($5.5.10^{-1}$ mbar) cycles.

Synthesis of β-$NaGd_{0.98}Er_{0.02}F_4$/$NaYbF_4$ NCs. The purified seeds solution is heated up under Ar to 290°C. Then, given quantities (Table S1) of YbTFA and NaTFA shell precursor solutions are mixed under inert atmosphere (glovebox) and introduced under Ar in a 10 mL disposable syringe equipped with a stainless steel needle, which is then fixed on a syringe pump. Then the combined shell precursor solution is slowly injected (250 μL/min) into the seeds solution. After injection, the temperature is maintained at 290°C for aging. After 60 minutes, the heating mantle is removed, and the flask is left to cool naturally to room temperature. The synthesized NCs are extracted and purified with a similar method as described for β-$NaGd_{0.98}Er_{0.02}F_4$ core NCs and stored in 1 mL toluene. Three different syntheses were performed with different Yb quantities giving rise to three different stock solutions of single-shell seeds (CSx with x = I, II, or III) dispersed in 1 mL toluene.

Synthesis of β-$NaGd_{0.98}Er_{0.02}F_4$/$NaYbF_4$/$NaGd_{0.99}Tm_{0.01}F_4$ double-shell NCs ($CS2_x$). β-$NaEr_{0.8}Yb_{0.2}F_4$/$NaYbF_4$/$NaGd_{0.99}Tm_{0.01}F_4$ NCs were synthesized by the controlled hot injection method. $NaEr_{0.8}Yb_{0.2}F_4$/$NaYbF_4$ CS NCs from the stock solutions (CS_I, CS_{II}, or CS_{III}) were used as the starting seeds. $CS2_x$ ($NaEr_{0.8}Yb_{0.2}F_4$/$NaYbF_4$/$NaGd_{0.99}Tm_{0.01}F_4$) NCs were synthesized with the same procedure as described for CS_x NCs. Quantities of seeds and shell precursor solutions are given in Table S1. Three different syntheses were performed with three different types of starting seeds (CS_I, CS_{II}, and CS_{III}) giving rise to three different stock solutions of double-shell seeds ($CS2_x$ with x = I, II, or III) dispersed in 1 mL toluene.

Synthesis of β-$NaGd_{0.98}Er_{0.02}F_4$/$NaYbF_4$/$NaGd_{0.99}Tm_{0.01}F_4$ /$NaYF_4$ triple-shell NCs ($CS3_x$). β-$NaEr_{0.8}Yb_{0.2}F_4$/$NaYbF_4$/$NaGd_{0.99}Tm_{0.01}F_4$/$NaYF_4$ NCs were synthesized by the controlled hot injection method. $NaEr_{0.8}Yb_{0.2}F_4$/$NaYbF_4$/$NaGd_{0.99}Tm_{0.01}F_4$ CS2 NCs from the three different stock solutions ($CS2_I$, $CS2_{II}$, or $CS2_{III}$) were used as the starting seeds. $CS3_x$ ($NaEr_{0.8}Yb_{0.2}F_4$/$NaYbF_4$/$NaGd_{0.99}Tm_{0.01}F_4$/$NaYF_4$) NCs were synthesized with the same procedure as described for CS_x and $CS2_x$ NCs. Quantities of seeds and shell precursor solutions are given in Table S1. Three different syntheses were performed with three different types of starting seeds ($CS2_I$, $CS2_{II}$, and $CS2_{III}$) giving rise to three different types of triple-shell ($CS3_x$ with x = I, II, or III) upconverting nanocrystals for color-tuning.

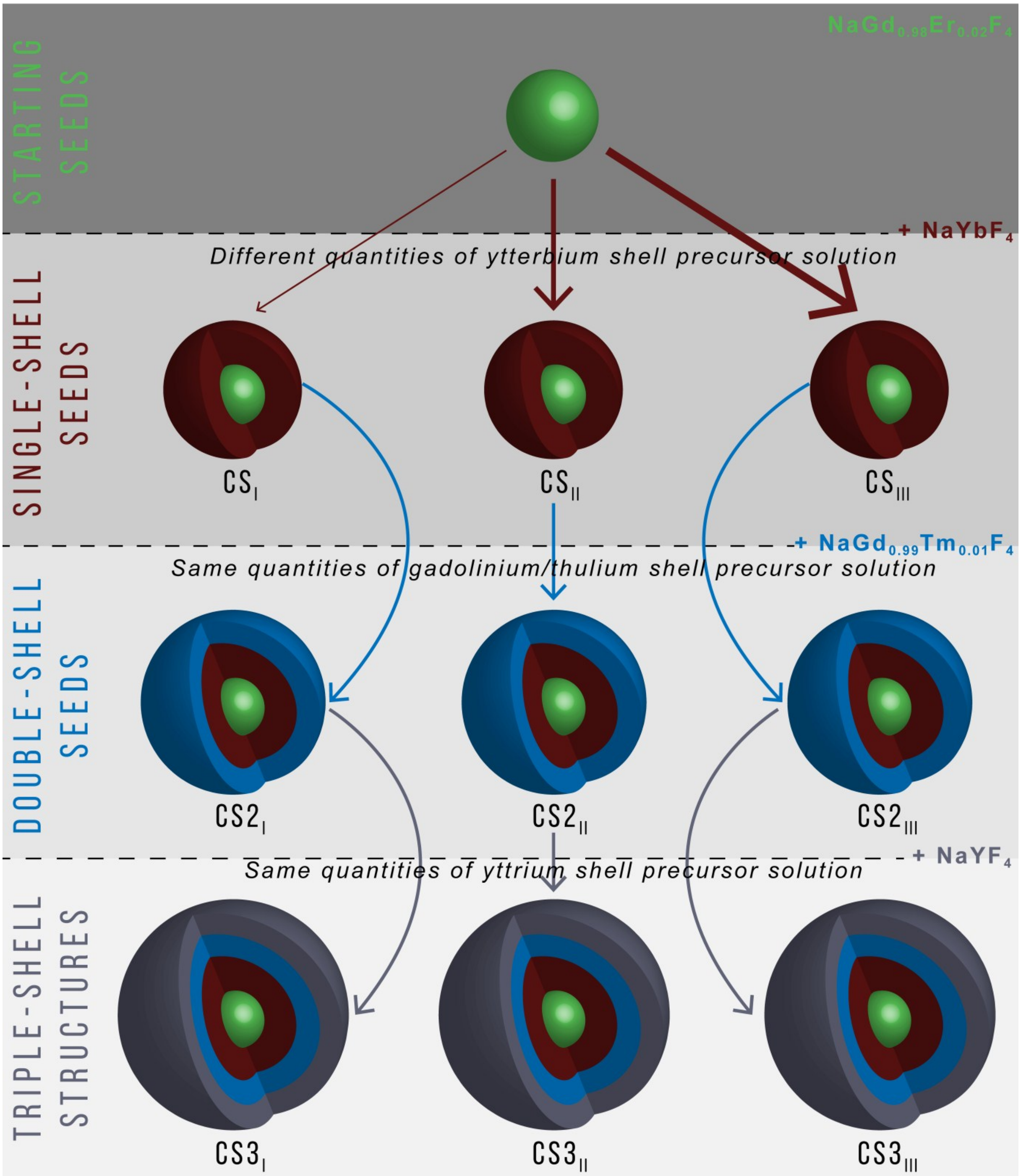

Figure S1. *Overview of the synthesis of triple-shell ($CS3_x$ with x = I, II, and III) upconverting nanocrystals (NCs) for color tuning. Note that the exact same starting core $NaGd_{0.98}Er_{0.02}F_4$ NCs have been used as the initial seeds for the synthesis of all $CS3_x$ NCs. Different quantities of ytterbium shell precursor solution were injected to prepare the single-shell (CS_x with x = I, II, and III) NCs. The latter were used as the starting seeds for the synthesis of double-shell ($CS2_x$ with x = I, II, and III) NCs for which the exact same quantity of gadolinium/thulium shell precursor solution was injected. Finally, CS2x NCs were used as the starting seeds for the synthesis of the final triple-shell ($CS3_x$ with x = I, II, and III) NCs for which the exact same quantity of yttrium shell precursor solution was injected.*

Single-shell (CS_x with x= I, II, and III) nanocrystals				
	Seeds	Seeds quantity (µL)	YbTFA quantity (µL)	NaTFA quantity (µL)
CS_{I}	$NaGd_{0.98}Er_{0.02}F_4$	500	4000	4000
CS_{II}		200	4000	4000
CS_{III}		100	4000	4000
Double-shell ($CS2_x$ with x= I, II, and III) nanocrystals				
	Seeds	Seeds quantity (µL)	GdTmTFA quantity (µL)	NaTFA quantity (µL)
$CS2_{I}$	CS_{I}	500	4000	4000
$CS2_{II}$	CS_{II}	1000	4000	4000
$CS2_{III}$	CS_{III}	1000	4000	4000
Triple-shell ($CS2_x$ with x= I, II, and III) nanocrystals				
	Seeds	Seeds quantity (µL)	YTFA quantity (µL)	NaTFA quantity (µL)
$CS3_{I}$	$CS2_{I}$	800	4000	4000
$CS3_{II}$	$CS2_{II}$	600	4000	4000
$CS3_{III}$	$CS2_{III}$	800	4000	4000

Table S1. *Nature of seeds and shell growth solutions as well as their relative quantities used for the synthesis of triple-shell ($CS3_x$ with x = I, II, and III) upconverting nanocrystals.*

7. Transmission electron microscopy (TEM) and scanning transmission electron microscopy (STEM).

Sample preparation. Transmission electron microscopy (TEM) samples were prepared (room temperature, air) by drop-casting 10 μL of diluted suspension of the NCs dispersed in toluene onto an ultrathin carbon film (2 nm) on holey carbon support film mounted on 400 μm mesh Cu grid (Ted Pella Inc.).

Instruments. The size, morphology and structure of nanoparticles were investigated by high-resolution (HR) TEM, selected-area electron diffraction (SAED) and high-angle annular dark-field (HAADF) scanning transmission electron microscopy (STEM) conducted with an aberration-corrected FEI Titan 80-300 microscope at 300 keV electron energy and a FEI Osiris ChemiSTEM microscope at 200 keV.

High-resolution transmission electron microscopy (HRTEM) and selected-area electron diffraction (SAED). HRTEM images were evaluated by calculating their two-dimensional (2D) Fourier transform (FT) patterns, which yields information on the crystal structure (lattice parameters and crystal symmetry) of single nanocrystals. The analysis was performed by comparing the experimental 2D FT patterns and calculated diffraction patterns, where the latter were obtained by using the JEMS (Java version of the electron microscopy simulation) software.[3] The zero-order beam (ZB) is indicated in the 2D FT patterns. SAED patterns of nanocrystals ensembles have been alternatively used to investigate their crystal structure.

8. Chemical information from transmission electron microscopy.

Chemical information was obtained by HAADF-STEM combined with energy-dispersive X-ray spectroscopy (EDXS). The experiments were carried out with a FEI Osiris ChemiSTEM microscope, which is equipped with a Bruker Quantax system (XFlash detector) for EDXS. EDX spectra are quantified with the FEI software package “TEM imaging and analysis” (TIA) version 4.7 SP3. Using TIA, element concentrations were calculated on the basis of a refined Kramers' law model, which includes corrections for detector absorption and background subtraction. For this purpose, standard-less quantification (theoretical sensitivity factors) without thickness correction was applied. The quantification of Na-, F-, Y-, Gd-, Yb-, Tm- and Er-content from their EDX spectra (line or area scans) was performed by evaluating the intensities of the F-$K_{\alpha1}$ line, Na-K series, Y-L, Gd-L, Yb-L, Tm-L, and Er-L series. We noted that X-ray lines of Cu (K- and L-series) from the grid, Gd-M, Er-M, Tm-M, and Yb-M series from nanocrystals, as well as the C-$K_{\alpha1}$ line from the amorphous carbon substrate were always present in the EDXS spectra. In addition Si-K and O-$K_{\alpha1}$ lines result from SiO_2 contamination of the TEM specimens.

Average chemical composition (area scans). EDX spectra obtained by scanning rectangular areas (nanocrystals ensembles) were acquired. The measured Na and F concentrations are a sum of their real concentration within NCs and their concentrations on the substrate under the nanocrystals. Hence, the Na/F concentrations on the substrate were determined and subtracted from the Na/F concentrations measured from the area scans to extract real nanocrystal concentrations. For this purpose, EDXS area scans were also acquired and quantified on particle-free regions close to the investigated areas.

Local chemical composition (line scans). Concentration profiles of different elements within a single nanocrystal were obtained from EDX spectra acquired along a line through the center of the corresponding NC. The EDXS line profiles were taken with a probe diameter of 0.5 nm and a distance of about 1 nm between two measuring points along the line. In analogy to area scans, the Na and F concentrations on the substrate under the nanocrystal were determined and subtracted from the total Na/F concentrations measured within the corresponding nanocrystal. In this case, the Na/F concentrations on the substrate were calculated by linear interpolation of the Na/F concentrations measured along the same EDXS line scan but on regions of the substrate exceeding the nanocrystal limits on both sides (left and right). Regarding the quantification of the EDX spectra of single core-shell nanocrystal, one has to keep in mind that the obtained compositions are averaged along the electron-beam direction. In other words, the whole volume along the electron trajectory contributes to the detected X-ray signal. To determine the composition of different regions of single- and multi-shell nanocrystals, a procedure was developed and is outlined elsewhere.[4]

9. Optical spectroscopy.

The photoluminescence parameters of the upconversion emission were measured in a home-built optical system. As an excitation source a 980 nm laser diode (Thorlabs L980P200) mounted in a temperature stabilized mount (TCLDM9, Thorlabs) and driven by an ITC4001 laser diode controller was used. The adjustment of the laser power was done by a controlled rotatable neutral density filter (Thorlabs). Absolute upconversion quantum yield (UCQY) values were measured according to the 3M procedure, first described by de Mello.[5,6]

For the UCQY measurements, the laser beam was additionally focused by a lens having a 15 cm focal distance and directed into the integrating sphere (IS) (Labsphere) with a 15 cm diameter. The beam size on the sample was measured with a Scanning Slit Optical Beam Profiler (BP209-IR/M, Thorlabs). For calculations of the irradiation intensity, 4-sigma beam diameters were used. The optical Y-fiber (Thorlabs) was used to collect the emission from the IS, which was then transferred to CCD spectrometers (CSS200, Thorlabs and AvaSpec-2048x64-TEC, Avantes). The measurement of absorption (measurement of the laser at the direct and indirect excitation of the sample plus empty sphere) was performed with the CCS200 spectrometer, whereas the measurement of the upconversion emission (usually several orders less in magnitude for NCs) was performed with the AvaSpec-2048x64-TEC spectrometer (suppression of the excitation radiation by a short pass filter SEM-

FF01-950/SP-25, Semrock). All raw spectra were re-calculated to the power spectra using an integration time value. The spectral response calibration of the whole detection system and cross-calibration of both spectrometers were done using an irradiance calibration lamp (HL-3plus-INT-CAL, Ocean Optics) and the correction was further applied to the power spectra. All UCQY measurement routines were automatized using Labview programs.

For the measurements of emissive level lifetimes, a TCSPC/MCS board (Timeharp 260, PicoQuant) was used. Modulation of the laser diode was performed with a built-in function generator of the laser driver. In order to detect rise and fall times of the upconversion emission, the TTL signal from the laser diode controller was delayed by the use of delay generator (DG645, Stanford Research Systems). The spectral separation of the photoluminescence was done with a double monochromator (DTMS300 Monochromator, Bentham). The detection of photons at specific wavelengths in the visible region was performed by counting PMT (R928P, Hamamatsu, mounted in cooling housing from Horiba), whereas for the detection of photons in the infrared region, an IR photon counter (ID220, IDquantiq) was used.

10. Supplementary figures

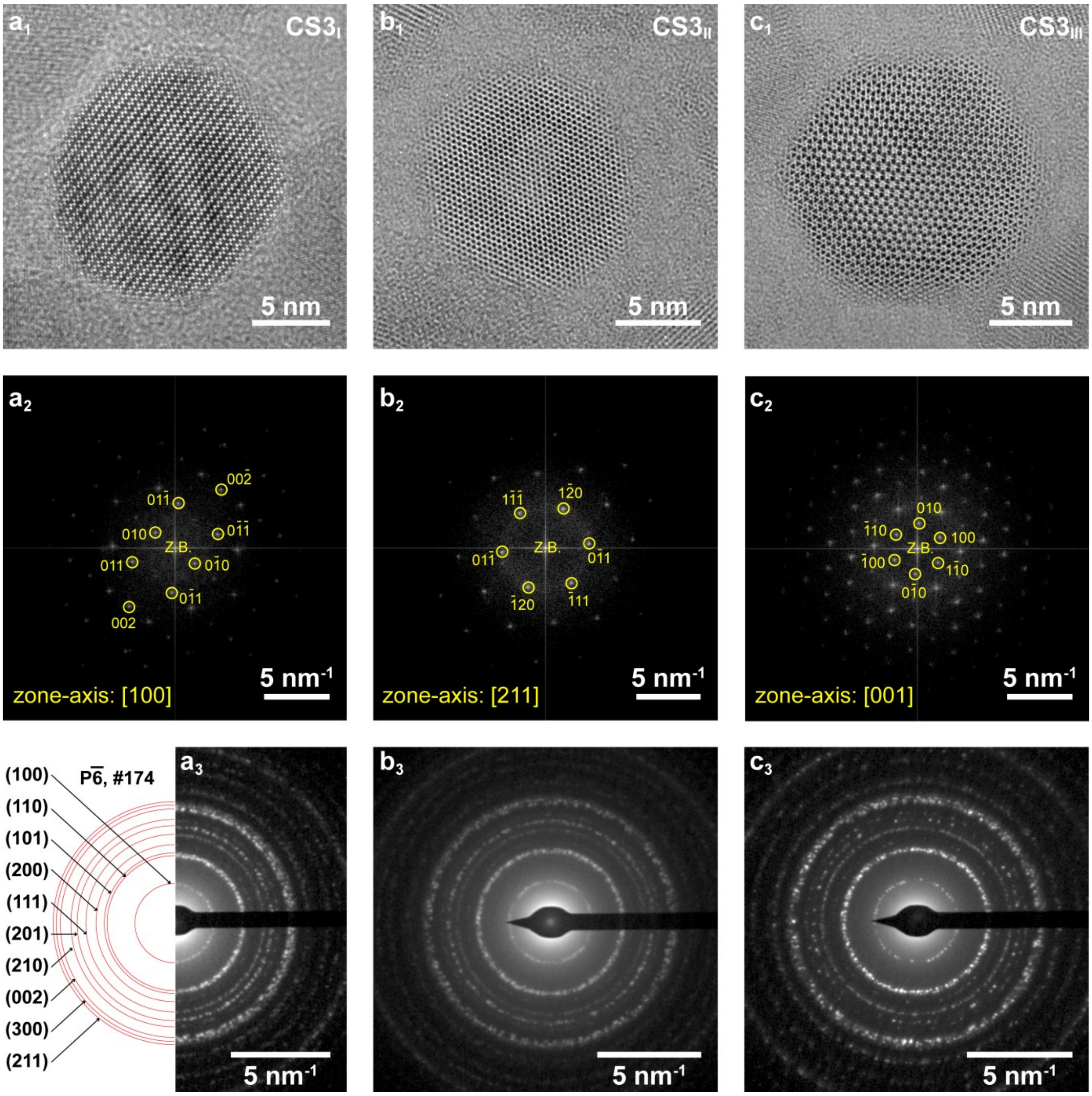

Figure S2. *High-resolution transmission electron microscopy (HRTEM) micrographs (top row) and their corresponding Fourier transforms (middle row), and selected area electron diffraction (SAED) patterns* of nanocrystal (NC) ensembles *(bottom row) of CS3$_I$ (a$_1$-a$_3$), CS3$_{II}$ (b$_1$-b$_3$), and CS3$_{III}$ (c$_1$-c$_3$) upconverting NCs. For Fourier transform patterns, the zone-axis is given (bottom left). The indexing of the SAED pattern of CS3$_I$ NCs (exact same indexing for CS3$_{II}$ and CS3$_{III}$) is superimposed for clarity. Note that the indexing is in perfect agreement with the formation of the pure hexagonal phase (P$\bar{6}$, #174) with no trace of the cubic phase.*

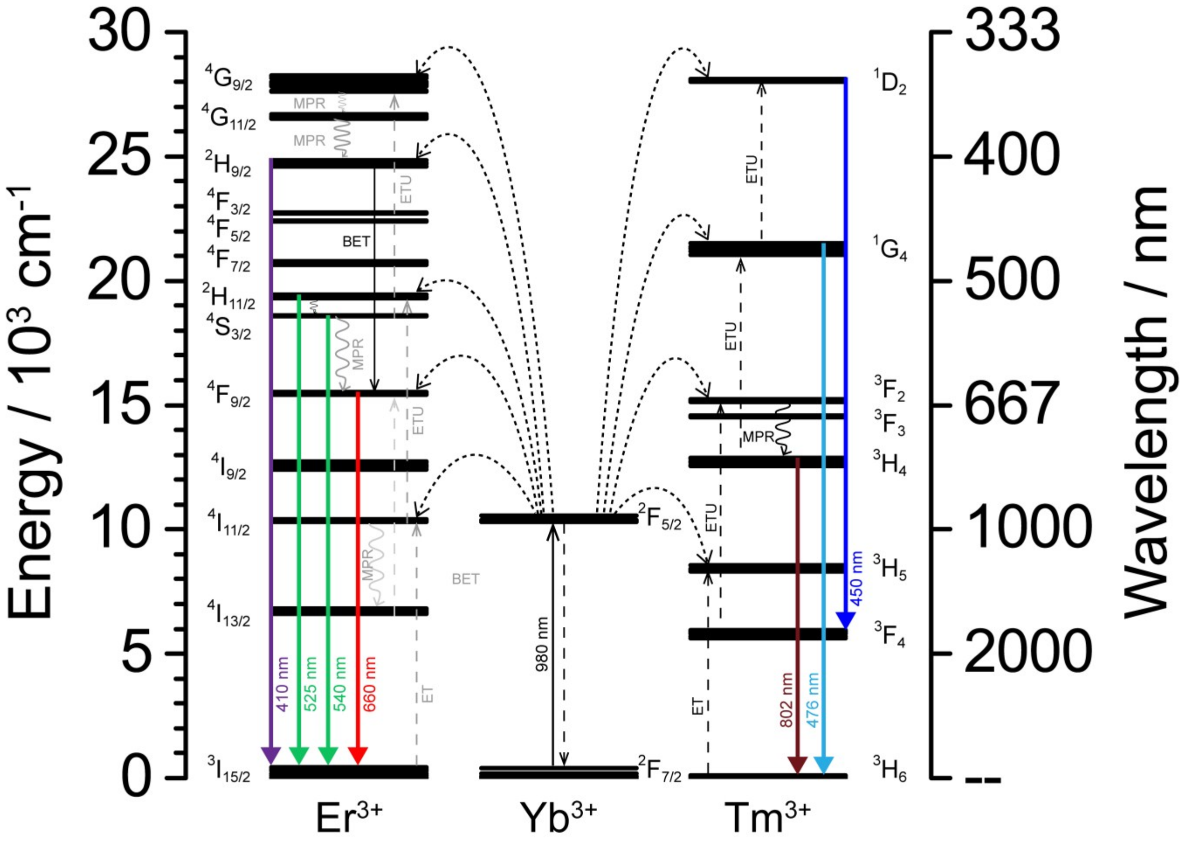

Figure S3. *Partial electronic energy level diagram for trivalent erbium, ytterbium, and thulium ions. The main radiative transitions and their corresponding wavelengths are indicated as well as typical energy transfer mechanisms between the sensitizer and activators. ET = Energy Transfer, ETU = Energy Transfer Upconversion, MPR = Multi-Phonon Relaxation, BET = Back Energy Transfer.*

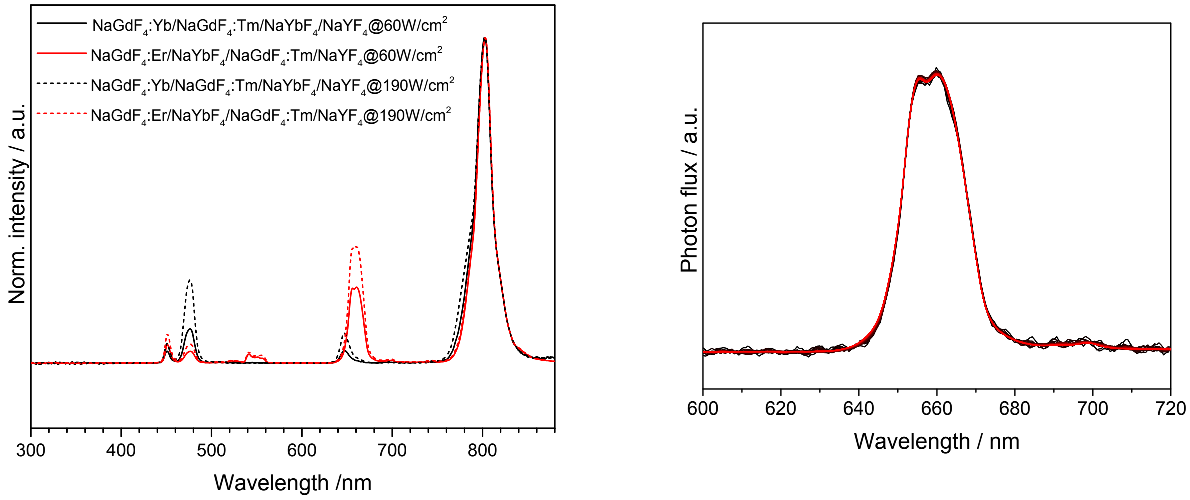

Figure S4. *Emission spectrum of triple-shell (Red: $CS3_{III}$; Black: $NaGdF_4$:Yb/$NaGdF_4$:Tm/$NaYbF_4$/$NaYF_4$) nanocrystals (left) synthesized with the same protocol as for the samples described in the main ($CS3_{III}$ NCs). Solid and dashed lines show the emission spectra with power densities of 60 and 190 W/cm^2, respectively. Normalized power-dependent (10 to 300 W/cm^2) emission spectra (red spectral region only) of $CS3_{III}$ nanocrystals.*

In order to check the influence of Tm^{3+} on the red emission region, triple-shell $NaGdF_4$:Yb/$NaGdF_4$:Tm/$NaYbF_4$/$NaYF_4$ NCs were synthesized. As can be seen on the corresponding emission spectrum (Figure S4 – left), there is indeed a weak emission peak at 649 nm, which is due to the $^1G_4 \rightarrow {}^3F_4$ transition (overlapping with the red emission from Er^{3+}). The power-dependent spectra of $CS3_{III}$ NCs in the red region with no show no alteration of the shape of the emission peak (Figure S4 – right). This indicates that the Tm^{3+} contribution to the red emission in $CS3_x$ NCs is negligible.

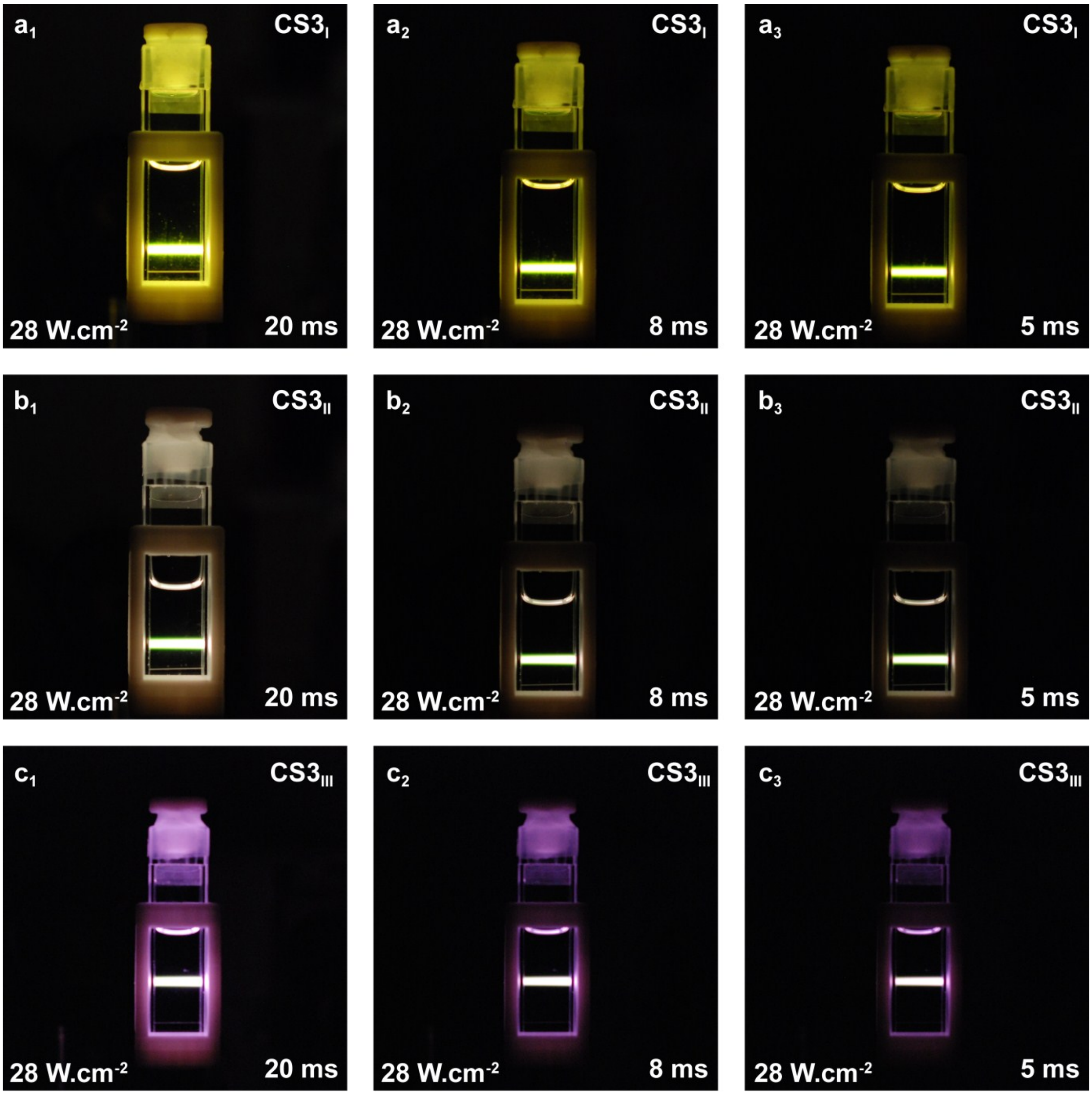

Figure S5. *Photographs of the as-prepared $CS3_I$ (a_1-a_3), $CS3_{II}$ (b_1-b_3), and $CS3_{III}$ (c_1-c_3) upconverting nanocrystals under 980 nm excitation at 28 $W.cm^{-2}$. All photographs were taken with a digital camera Nikon D80 equipped with a Micro-Nikkor objective (60mm f/2.8). All photographs were taken with the same ISO and aperture photography settings (ISO 800, f/5.6) but different shutter speeds, namely 1/50 s (first column), 1/125 s (middle column), and 1/200 s (right column).*

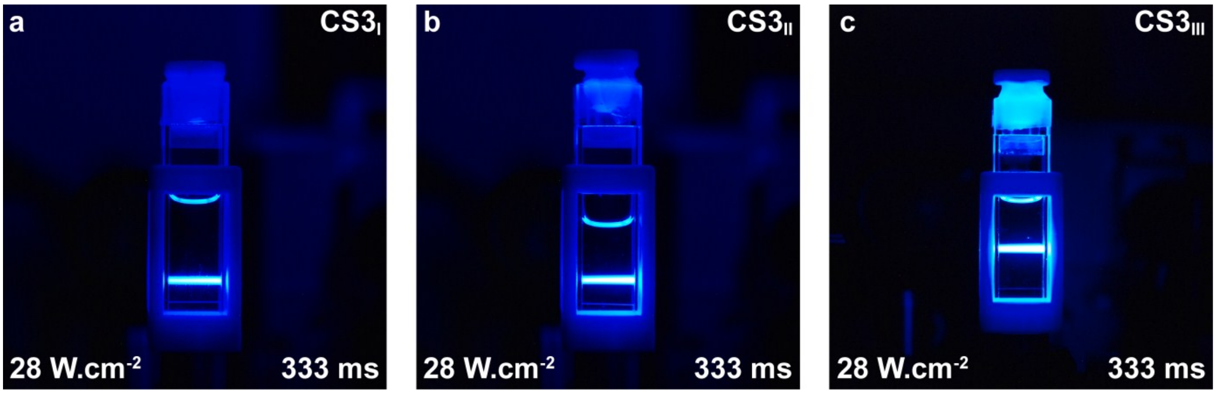

Figure S6. *Photographs of the as-prepared CS3$_{I}$ (a), CS3$_{II}$ (b), and CS3$_{III}$ (c) upconverting nanocrystals under 980 nm excitation at 28 W.cm^{-2}. All photographs were taken with a digital camera Nikon D80 equipped with a Micro-Nikkor objective (60mm f/2.8). All photographs were taken with the same ISO, shutter speed, and aperture photography settings: ISO 800, 1/3 s, f/5.6. A shortpass filter (500 nm) was inserted in front of the camera objective.*

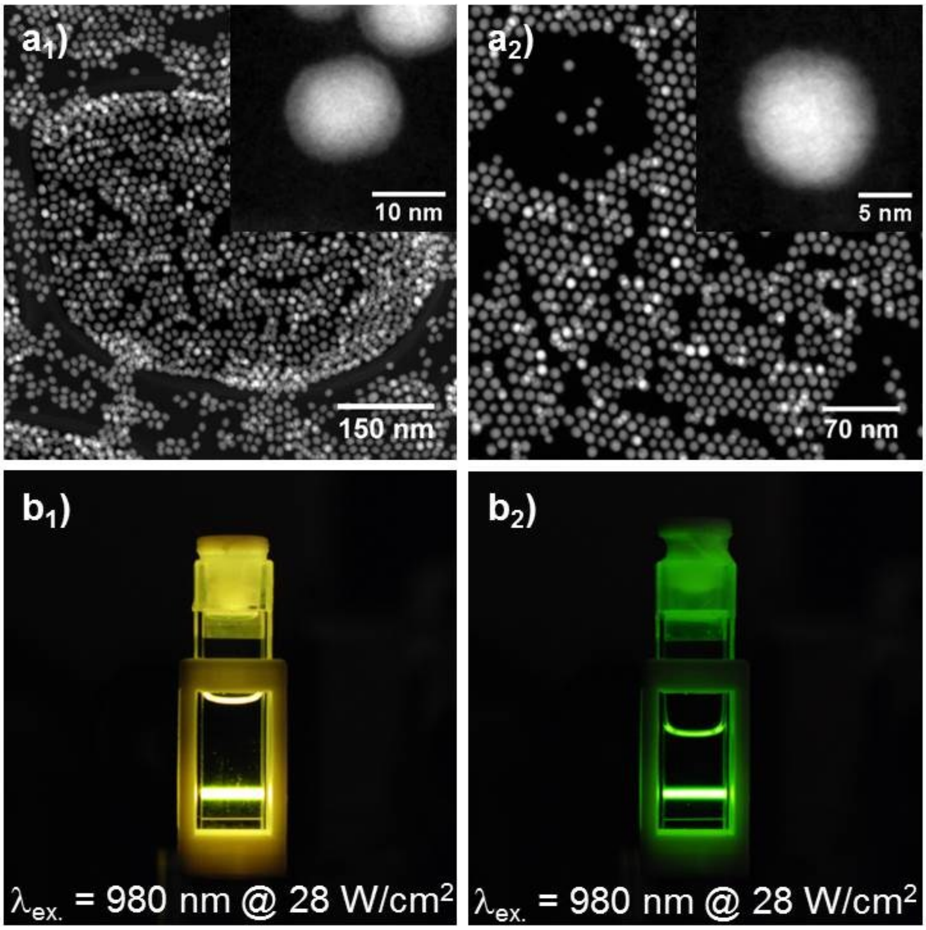

Figure S7. *Color-tuning in triple-shell NaGdF$_4$:Er / NaYbF$_4$ / NaGdF$_4$:Tm / NaYF$_4$ NCs can be reached by changing the shell deposition method (left vs. right columns). STEM micrographs are shown (top row) together with the photographs (bottom row) of the corresponding colloidal suspensions (2.5 wt.% solution in toluene) under near-infrared excitation (980 nm at 28 W/cm^2). All photographs were taken with a digital camera Nikon D80 equipped with a Micro-Nikkor objective (60mm f/2.8). All photographs were taken with the same ISO, shutter speed, and aperture photography settings, namely ISO 800, 1/50 s, f/5.6.*

It was recently demonstrated that the magnitude of the intermixing effect was different as a function of the shell deposition method.[7] The effect of different amounts of intermixing was checked by changing the deposition method. The same triple-shell structures as reported in the main text (NaGdF$_4$:Er/NaYbF$_4$/NaGdF$_4$:Tm/NaYF$_4$) were synthesized from the exact same starting seeds (i.e. same synthesis batch for the NaGdF$_4$:Er core NCs) but the shells (of the same chemical composition) were deposited by two different shell deposition methods (Figure S7). The first method (Figures S7 a$_1$-b$_1$ - as described in the text) is based on the use of trifluoroacetates as the starting precursors whereas the second method relies on the use of lanthanide acetates, ammonium fluoride, and sodium hydroxide.[7] These different shell deposition methods indeed give rise to different upconversion colors.

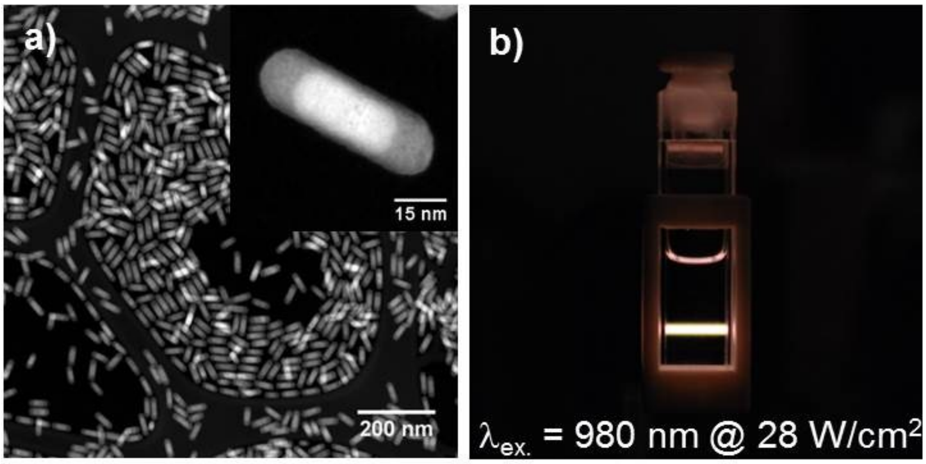

Figure S8. *Color-tuning in triple-shell $NaGdF_4$:Er / $NaYbF_4$ / $NaGdF_4$:Tm / $NaYF_4$ NCs can be reached by changing the size of the starting seeds. The STEM micrograph is shown (a) together with the photograph (b) of the corresponding colloidal suspension (2.5 wt.% solution in toluene) under near-infrared excitation (980 nm at 28 W/cm^2). All photographs were taken with a digital camera Nikon D80 equipped with a Micro-Nikkor objective (60mm f/2.8). The photograph was taken with the same ISO, shutter speed, and aperture photography settings, namely ISO 800, 1/50 s, f/5.6. The triple-shell NCs were synthesized with the same shell deposition method as for NCs shown in Figure R3 (a_2-b_2).*

The same triple-shell structure as reported in the main text ($NaGdF_4$:Er/NaYbF4/NaGdF4:Tm/NaYF4) and synthesized by the same shell deposition method as the sample reported in Figure S7 (a_2-b_2) but with different starting seeds (bigger and slightly anisotropic seeds) is characterized by a different emission color (Figure S8).

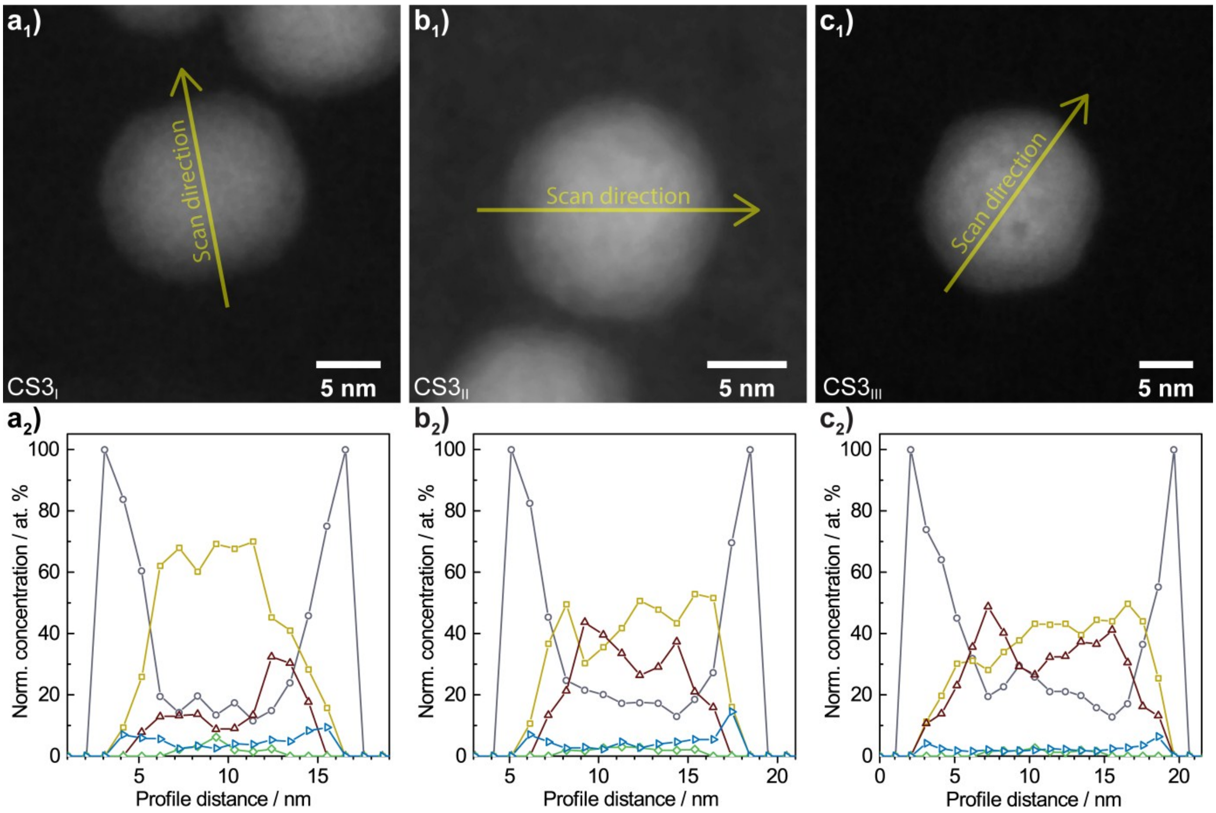

Figure S9. *High-angle annular dark-field scanning transmission electron microscopy (HAADF-STEM) micrographs with yellow arrows indicating the energy dispersive X-ray spectroscopy (EDXS) scan directions of individual CS3$_{I}$ (a_1), CS3$_{II}$ (b_1), and CS3$_{III}$ (c_1) nanocrystals (NCs). Corresponding raw concentration profiles before correction (gadolinium – dark-yellow; erbium – green, ytterbium – dark-red, thullium – blue, and yttrium - gray) of individual CS3$_{I}$ (a_2), CS3$_{II}$ (b_2), and CS3$_{III}$ (c_2) NCs.*

11. References

[1] Nanotechnology **2008**, 19, 345606.

[2] Nature Protocols **2014**, 9, 1634.

[3] http://www.jems-saas.ch

[4] RSC Advances **2012**, 2, 9473, Advanced Materials **2019**, In Press, DOI: adma.201900623.

[5] Advanced Materials **1997**, 9, 230.

[6] Laser & Photonics Reviews **2012**, 6, 802.

[7] Journal of Materials Chemistry C 2019, 7, 1164.